In Silico Pharmacology (2021) 9:19
https://doi.org/10.1007/s40203-021-00079-w

ORIGINAL RESEARCH

In silico analysis of STX2a-PE15-P4A8 chimeric protein as a novel immunotoxin for cancer therapy

Maryam Keshtvarz[1] · Jafar Salimian[2] · Jafar Amani[3] · Masoumeh Douraghi[1] · Ehsan Rezaie[4]

Received: 17 April 2020 / Accepted: 19 January 2021

Abstract

Today, the targeted therapies like the use of immunotoxins are increased which targeted specific antigens or receptors on the surface of tumor cells. Fibroblast growth factor-inducible 14 (Fn14) is a cytokine receptor which involves several intercellular signaling pathways and can be highly expressed in the surface of cancer cells. Since the cleavage of enzymatic domain of *Pseudomonas exotoxin A* (PE) occurs in one step by furin protease, we fused enzymatic subunit of Shiga-like toxin type 2a (Stx2a) with domain II and a portion of Ib of PE to increase the toxicity of Stx. Then, we genetically fused the Fv fragment of an anti-Fn14 monoclonal antibody (P4A8) to STX2a-PE15 and evaluated the STX2a-PE15-P4A8 chimeric protein as a new immunotoxin candidate. In silico analysis showed that the STX2a-PE15-P4A8 is a stable chimeric protein with high affinity to the Fn14 receptor. Despite, the STX2a-PE15-P4A8 can be bind to the B cell receptor, but it has been weakly presented by major histocompatibility complex molecules II (MHC-II). So, it may have a little immunogenicity. On the basis of our in-silico studies we predict that STX2a-PE15-P4A8 can be a good candidate for cancer immunotherapy.

Keywords Cancer · Exotoxin A · Fn14 receptor · P4A8 · STX2a

✉ Jafar Amani
jafar.amani@gmail.com

✉ Masoumeh Douraghi
mdouraghi@tums.ac.ir

Maryam Keshtvarz
mkeshtvarz@gmail.com

Jafar Salimian
jafar.salimian@gmail.com

Ehsan Rezaie
rezaie.ehs@gmail.com

1 Division of Microbiology, Department of Pathobiology, School of Public Health, Tehran University of Medical Sciences, Tehran, Iran

2 Chemical Injuries Research Center, Systems Biology and Poisonings Institute, Baqiyatallah University of Medical Sciences, Tehran, Iran

3 Applied Microbiology Research Center, Systems Biology and Poisonings Institute, Baqiyatallah University of Medical Sciences, Vanak Sq. Molasadra St., P.O. Box 19395-5487, Tehran, Iran

4 Molecular Biology Research Center, Systems Biology and Poisonings Institute, Baqiyatallah University of Medical Science, Tehran, Iran

Abbreviations

Stx	Shiga toxin
Stx2a	Shiga-like toxin type 2a
PE	*Pseudomonas exotoxin A*
MHC-II	Major histocompatibility complex molecules II
Fn14	Fibroblast growth factor-inducible 14
ScFv	Single chain fragment variable
VH	Heavy *chain variable* domain
VL	Light *chain variable* domain
E.coli	*Escherichia coli*

Introduction

Cancer is one of the leading causes of death in all regions of the world. As predicted by the World Health Organization (WHO), the cancer mortality rate will reach almost 80% in 2030, especially in low and moderate income countries (Siegel et al. 2019). Surgery, chemotherapy, and radiation therapy are common treatments for cancer. Nevertheless, the high cancer death rate is indicating that the mentioned methods are not very effective (Cancer 2014; Zauber et al. 2012).

Today, targeted therapies such as immunotoxins are used as new treatment by targeting the specific antigens or receptors on the surface of cancer cells. Immunotoxins are

Published online: 10 February 2021

made of a whole antibody or antibody fragment as targeting moiety with a component of the toxin. The antibody facilitates the entry of toxin via receptor-mediated endocytosis and consequently results in the death of cells through toxin activity (Kreitman 2006).

Most potent toxins are proteins derived from bacteria, fungal or plants and may inhibit protein synthesis enzymatically, and lead to cell death. The AB toxins are two-component molecules. *Pseudomonas*exotoxin A (PE) is one of the potent AB toxins and often used in the immunotoxins structure for targeted cancer therapy; owing to its easy production in *Escherichia coli,* stability, and significantly lower immunogenicity. PE is a 613-amino acid protein consisting of three domains; domain I (cell-binding domain), domain II (translocation domain), and domain III (catalytic domain). The N-terminal domain I include domains Ia (residues 1–252) and Ib (365–404), while domain II (253–364) fits to residues between domains Ia and Ib and the rest of the residues in C-terminal comprise domain III (405–613). Domain Ia of PE is the receptor-binding domain which enables the entry of domain II and III into the cell. Domain II is involved in toxin translocation and intracellular trafficking, and domain III catalyzes ADP ribosylation, inactivate elongation factor 2, inhibits protein synthesis, and finally leads to cell death (Michalska and Wolf 2015). In addition, Domain III requires a part of domain Ib for its full catalytic activity. In endosome, PE cleavage occurs by furin in a region on domain II and then the enzymatic fragment of toxin is transported to the Golgi apparatus, endoplasmic reticulum (ER) and cytoplasm; a location on which protein synthesis is inhibited.

Different forms of toxins for applying in immunotoxins have been designed. PE40 is produced by deletion of domain Ia whereas further deletion of a portion of domain Ib (residues 390–404) results in another molecule named PE38 (Kawa et al. 2011; Matar et al. 2012; Tredget et al. 2004). The PE38 has been applied in many immunotoxins (Hassan et al. 2014; Keshtvarz et al. 2017; Rezaie et al. 2020a, b) but this engineered toxin in some cases has been highly immunogenic and lead to the production of the anti-drug antibodies against the PE38 moiety (Alewine et al. 2015). Deletion of a portion of domain Ib (residues 390–404) and all residues of domain Ia, and III result in another known molecule; PE15.

Another type of the AB toxins are Shiga-like toxins that are produced by *E.coli* O157:H7. Shiga-like toxins are divided into the two groups on the basis of their immunological properties, stx1 and stx2. Shiga-like toxin 2 (Stx2) has about *55%* identical with stx1 (Kawa et al. 2011). They are composed of a pentameric binding subunit (stxB) that is non-covalently attached to an enzymatic subunit namely A subunit (stxA). After binding of the Stx to its receptor (Globotriaosylceramide, known as Gb3), Stx is cleaved into two parts; active A1 subunit and A2-B pentamer complex. StxA1 is still connected to StxA2-B5 through a disulfide bond and is transported to the Golgi apparatus, endoplasmic reticulum (ER). In the ER, StxA1 can be completely separated from A2-B5 after reduction of the disulfide bond, and then enters into the cytoplasm. In the cytoplasm, Stx A1 inhibits protein synthesis through the removal of a single adenine residue from the 28S rRNA and leads to apoptosis.

Fn14, fibroblast growth factor 14, can activate several intracellular signaling pathways like the nuclear factor-κB (NF-κB) pathway. Fn14 expression is comparatively low on normal tissues except lymphocyte cells, but high expression of Fn14 is demonstrated in the majority of tumor cell types such as breast, pancreatic, melanoma, and lung cancer. Therefore, Fn14 can be considered as a candidate for ligand-targeted therapeutics. Furthermore, the Fn14 expression level is correlated with tumor progression and resistance to standard therapies (Brown et al. 2003; Whitsett et al. 2012; Winkles 2008; Zhou et al. 2011). We selected Fn14 monoclonal antibody P4A8 (anti-Fn14) as a potentially important target for cancer immunotherapy.

In the present study, we used in silico techniques to design and compare a recombinant immunotoxin for cancer therapy. The *stx2a(A1)-pe15-p4a8* chimera was designed and evaluated through bioinformatics methods. Since the cleavage of enzymatic domain of PE occurs in one step by furin, we fused A1 subunit of STX2a (enzymatic domain) to domain II and a portion of Ib of PE to increase toxicity of Stx. The *stx2a(A1)-pe15-p4a8* gene was optimized in a suitable host to express and predict secondary RNA structures, as well as physico-chemical and structural properties of the modeled protein, its stability, cleavage sites, and the stimulation of cellular and humoral immune responses.

Materials and methods

Sequence analysis

The amino acid sequences of heavy (VH) and light (VL) chain variable of P4A8 antibody were retrieved from Patent *EP2294089A2*, and the amino acid sequences of STX2a (Q2ACF1) and PE (P11439) were obtained from online banks including Swiss-Prot and Gen Bank.

Design and optimization of the chimeric construct

DNAsis MAX (Hitachi Software), java codon optimization tool (JCat) server (http://www.jcat.de/), codon usage server (http://wwwgeneinfinity.org/sp/sp_codonusage.htm), OPTIMIZER server (http://genomes.urv.es/OPTIMIZER), and gene script server (http://www.genscript.com/) were used

for optimizing the sequence of chimeric construct based on *Escherichia coli* codon usage data bank.

Prediction of RNA secondary structure

RNA secondary structure of the chimeric protein before and after the gene optimization was predicted using the "mfold server" (http://mfold.rna.albany.edu/). The results were re-examined with web servers such as RNAfold-ViennaRNA (http://rna.tbi.univie.ac.at/cgi-bin/RNAfold.cg) and predicate secondary structure (http://rna.urmc.rochester.edu/RNAstructure).

Analysis of physicochemical parameters of the chimeric protein

Physiological parameters of the chimeric protein such as molecular weight, Isoelectric point (pI), amino acid composition, atomic composition, extinction coefficient, estimated half-life, instability index, aliphatic index, and grand average of hydropathicity (GRAVY) were computed using PROTPARAM (http://web.expasy.org/protparam/) web server.

Protein solubility prediction

Solubility of the chimeric protein was evaluated through Recombinant Protein Solubility (http://www.biotechou.edu/) and SOSUI (http://harrier.nagahama-i-bio.ac.jp/sosui).

Protein secondary structure prediction

The secondary structure of the chimeric protein was predicated by web servers such as Chou-Fasman, GOR and Neural Network ver. 1.1 (cib.cf.ocha.ac.jp/bitool/MIX), GORIV (http://gor.bb.iastate.edu/), and PCI-SS (http://bioinf.sce.carleton.ca/PCISS/start.php) for checking the presence of alpha helix and beta platedsheets in the structure. Finally, the secondary structure of the chimeric protein was compared with the structure of native (PE38) protein.

Protein tertiary structure prediction

The three-dimensional (3D) structure of the chimeric protein was predicted from I-TASSER (http://zhanglab.ccmb.med.umich.edu/I-TASSER). The predicted PDB models were also vie-wed throughWD40-C3nd 4.3 or DS Visualizer, and ActiveX Control 4.0 software**.** ProSA(https://prosa.services.came.sbg.ac.at/prosa.php) and RAMPAGE (http://mordred.bioc.cam.ac.uk/rapper/rampage.php) web servers were used to identify the errors predicted in 3D structure and to analyze its reliability.

Prediction of cleavage sites

ProP 1.0 Server (www.cbs.dtu.dk/services/ProP) was used to predict peptidase cleavage sites and signal peptide cleavage sites in the native protein and synthetic chimeric protein.

Proteasomal cleavage sites and peptides binding affinity to Transporter associated with antigen processing (Kawa et al.) protein of the synthetic chimeric protein were computed using Netchop 3.1 (http://www.cbs.dtu.dk/services/NetChop/), TAPPred (http://www.imtech.res.in/raghava/tappred) servers. NetCTL-1.2 server used to predict the location and binding specificity of CTL epitopes in protein sequences.

Prediction of human B cell and T cell epitopes

Linear and conformational B cell epitopes were predicated using ABCpred (www.imtech.res.in/raghava/abcpred/) web server based on physico-chemical properties of the chimeric protein. BCPREDs (ailab.ist.psu.edu/bcpred),and Bepired (www.cbs.dtu.dk/services/BepiPred) web servers were also used for prediction of conformational B epitopes.

Then, DiscoTope 2.0 (www.cbs.dtu.dk/services/DiscoTope/) and CBTOPE (http://www.imtech.res.in/raghava/cbtope) web servers were used for predicting discontinuous B cell epitopes in 3D structures of the chimeric protein.

NetCTL 1.2 (www.cbs.dtu.dk/services/NetCTL/), EpiJen (www.ddgpharmfac.net/epijien) servers have been used to predict CTL epitopes. The IEDB (tools.immuneepitope.org), CTLPred (www.imtech.res.in/raghava/ctlpred), NetCTL 1.2 (www.cbs.dtu.dk/services/NetCTL), and Propred (www.imtech.res.in/raghava/propred) web servers were applied for identifying the MHC Class-I binding and MHC class-II epitopes, respectively.

Prediction of allergenic and antigenic properties of the chimeric protein

The presence of possible allergenic sites was predicted by AlgPred (www.imtech.res.in/raghava/algpred/) web server. AlgPred can predicate allergens according to the similarity of recognized epitopes with any region of protein. Moreover, the analysis of antigenicity of the chimeric protein was done using VaxiJen (www.ddg-pharmfac.net/vaxijen) antigen prediction server.

Evaluation of cellular and cytokine responses

To obtain deep knowledge about the formed immune responses against our construction, we predicted the

cellular and cytokine responses to the immunotoxin by C-IMMSIM simulator online server at http://150.146.2.1/C-IMMSIM.

Docking method for investigating the protein–ligand interactions

The interaction between the chimeric protein and the Fn14 receptor on tumor cells was done using Hex docking software, version 6.12 (http://www.loria.fr/~ritchied/hex/).

Results

Designing and optimizing of the chimeric construct

The composition of STX2a (166 aa), PE15 [Ib (25 aa), and II (112 aa)], and Fv portion of P4A8 [VL (111 aa) and VH (121 aa)] sequence was made by connecting the C-terminal of PE15, and the N-terminal of anti-Fn14 ScFv (single chain fragment variable) (STX2a-PE15-anti-Fn14 ScFv) using two proper linkers; ASGGPE and (G4S)3. After finding restriction cleavage sites in pET-28b plasmid, the *Bam*HI, and *Xho* I restriction sites were inserted in the 5′ and 3 ’ends of the chimeric sequence for sub cloning. In addition, the Hind III restriction site was added after the second linker (between PE15 and VL) (Fig. 1). Then, the amino acid sequence (561 aa) of the chimeric construct was back translated to nucleic acid and its codon bias and GC content was assessed based on the codon labeled *E.coli* K12 as a prokaryotic host for gene expression versus wild type gene by www.jcat.deserver. For optimization of the synthetic chimera, factors including prokaryotic ribosome binding sites, Cleavage Sites of Restriction Enzymes, and rho-independent transcription terminators, which may have a negative impact on the expression rate were deleted. CAI in the optimized gene and un optimized gene was 0.93 and 0.68, respectively. CAI of > 0.8 *is* considered as a high gene expression level in a proper host. The content of GC of the un optimized gene was 56.3% and reduced to 52.9% in the optimized gene (GC% of *E.coli* k12 is 50.7) (Supplementary Fig. 1). The NCBI accession number of *stx2a-pe15-P4A8* sequence is KJ866881.

Prediction of mRNA structure

Frothy five models of chimeric mRNA were predicted compared with forty one models of native gene. The 5′ end of native and chimeric genes was found in the beginning of pseudoknot and hairpin, respectively. Forming a hairpin loop structure is related to the stability of helix and loop regions, while loops like pseudoknot pairing with more bases are unstable. The best secondary structure of chimeric mRNA had more minimum free energy (ΔG = − 561.74 kcal/mol) than native mRNA (− 425.48 kcal/mol). Thermodynamic details of the 5′ end of the chimeric construct were illustrated in Table 1. The minimum free energy (ΔG) of the5′ end of the chimeric was < − 6 (− 6.60), which constrain the hairpin loop structure. According to the data in Table 1 and Supplementary Fig. 2, the chimeric construct has stability greater than native gene.

Analysis of the physicochemical parameters

Using the PROTPARAM web server, the physicochemical characteristics of the chimeric construct (561 aa) versus native protein (346 aa) was computed (Table 2). The acidity of the chimeric and native protein was indicated by TPI value; (TPI of the chimeric and native gene was 6.13 and 5.03, respectively). The amount of positively (Arg and Lys) charged residues in the both proteins was less than of

Table 1 Thermodynamic details related to 5′ end of the chimeric construct (*stx2a-pe15-P4A8*) mRNA

Structural element	ΔG(STX2a-PE15-P4A8)	Information (STX2a-PE15-P4A8)
External loop	− 1.20	5 ss bases and 1 closing helices
Stack	− 3.30	External closing pair is G_3-C_{1686}
Stack	− 2.40	External closing pair is G_4-C_{1685}
Stack	− 0.90	External closing pair is A_5-U_{1684}
Helix	− 6.60	4 base pairs
Interior loop	2.50	External closing pair is A_6-U_{1683}
Stack	− 2.10	External closing pair is C_{12}-G_{1677}

According to minimum free energy (ΔG) of 5′ end of the chimeric mRNA, the initial ATG is located in hairpin loop structure

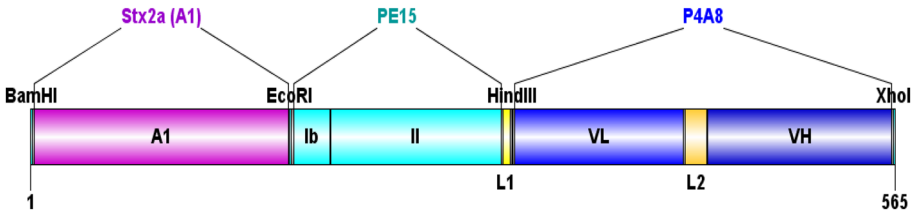

Fig. 1 A Schematic model of *STX2a (A1)-PE15*-P4A8 (VH and VL) construct fused together through Linker 1; ASGGPE and linker2; (G4S)3 for expression in *E.coli*. A1, enzymatic domain of Stx2a,; Ib, PE domain Ib; II, PE domain II

Table 2 Parameters calculated by Expasy'sProtParam tool

Sequence length	Mw	TpI	− R	+R	EC	II	AI	GRAVY
561	60,699.5	6.13	50	44	76,585	43.24	72.71	− 0.286 to 0.286
346,346	37,309.6	5.07	45	33	44,015	40.35	84.45	− 0.382

Mw molecular weight; *T pI* theoretical isoelectric point; *− R* number of negative charged residues; *+R* number of positive charged residues; *EC* extinction coefficient at 280 nm; *II* Instability index; *AI* Aliphatic index; *GRAVY* Grand Average Hydropathy

negatively (Asp and Glu) charged residues. The extinction coefficient of the chimeric and native protein at 280 nm was 76,585 and 44,015 M-1 cm^{-1}, which play an important role in protein–protein interaction.

Instability index is more than 40 and indicates that PE38-P4A8 protein is an unstable protein. The estimated half life of the both proteins was more than 10 h. Based on the predicted instability index, the ProtParam tool indicates that the chimeric construct and native protein are unstable with a value of 43.24 and 40.35, respectively. Aliphatic index of chimeric and native protein was 72.71 and 84.45, respectively. This high aliphatic index indicates that both proteins can be stable within a wide range of temperature. The low GRAVY index (−0.286 and − 0.382) of the chimeric and native protein indicates that both proteins are reactive in water. Moreover, ProtParam results showed that the percentage of Ser (11.6%) and Ala (12.4%) in the chimeric construct is higher than the other residues (Table 1).

Prediction of the solubility of the chimeric protein

Recombinant protein solubility predicated that the chance of solubility of the chimeric protein is 0% during expression in *E. coli* host.

Prediction of the secondary structure of the chimeric protein

Using GOR IV server, the secondary structure of the chimeric protein versus native protein (PE38) was predicted (Supplementary Fig. 3). Random coil, extended strand and alpha helix are structural contents of the chimeric and native protein. Also, the predicted structures of the linkers were coil that could significantly separate different segments of the proteins.

Prediction of Tertiary structure of the chimeric protein

Using the I- TASSER web server, five possible models for tertiary structure of the chimeric protein were predicted (Supplementary Fig. 4). The Z-score of the best predicted 3D model was −4.33. C-score, TM-score, and RMSD of the best predicted model were − 1.66, 0.51 ± 0.15, and 11.5 ± 4.5 Å, respectively. The C-score is used to estimate the quality of predicted models and its normal range is − 5 to 2. The model 5 with the highest C-score was the best predicted model. The TM-score and RMSD were used to assess the accuracy of the models and structural similarity.

Evaluation of model stability

The structural stability of the synthetic chimeric protein (STX2a-PE15-P4A8) was assessed based on hypothetical designated proteins using the RAMPAGE web server. The Ramachandran plot showed that among the 561 amino acid residues, 408 (72.8%) residues were in favoured regions while 27.3% of residues were in the allowed and/or outlier regions (Supplementary Fig. 5).

DS Visualizer software used to view predicted PDB models. As shown in Fig. 2 3D model showed that the chimeric protein is made of four separate parts including STX2a (166 aa), Ib and II domain of PE15 (25aa and 112aa respectively), VL (111aa), and VH (121aa). The most important region of the chimeric protein is STX2a with cytotoxic activity. STX2a-PE15 binds to the Fn14 receptor on the tumor cells through VH and VL of P4A8, and PE15 facilitates the translocation of STX2a in the cytosol. STX2a is able to inhibit of the protein synthesis and cause cell death (Fig. 2).

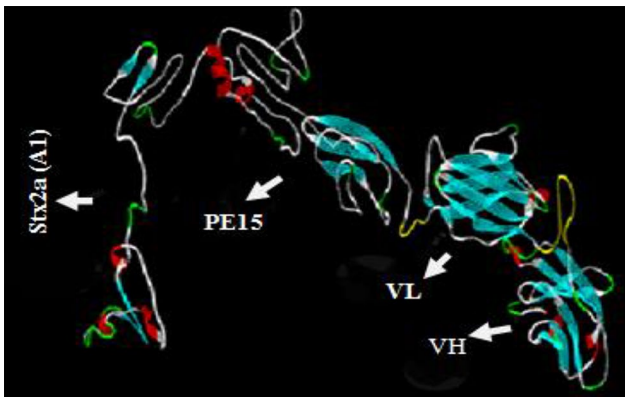

Fig. 2 Four dimensional view of STX2a-PE15-P4A8 chimeric protein. STX2a, PE15, VL, and VH of anti-Fn14 made four separated domains. Linkers were marked in yellow font

Prediction of cleavage sites

Using NetChop 3.1 (C-term 3.0 version) server, 177 and 133 cleavage sites were identified in the chimeric and native proteins, respectively. These results showed that replacing domain III by STX2a didn't affect in the cleavage sites of Ib and II domains. Prediction of binding affinity of TAP binder in the chimeric protein was done by TAPPred server. There were 35 TAP binding sequences with high affinity in the chimeric protein that only its seven sequences were similar to TAP binding sequences in the native protein (Table 3).

Prediction of T and B cell epitopes

Cytotoxic T lymphocyte (CTL) epitopes in the STX2a-PE15-P4A8 and PE38 protein were predicted using NetCTL1.2 server as proteasomal cleavage, TAP transport efficiency, and MHC class I binding. 26 MHC ligands and 553 peptides in the chimeric protein (Table 4) and 3 MHC ligands and 339 peptides in the native protein (data not shown) were identified. Moreover, the results indicated that there was no difference between epitopes identified in PE15 of the chimeric protein in front of the position in the native protein.

Using IEDB server prediction of T cell epitopes of the chimeric and native protein for MHC-I and MHC-II human motifs were done. There was no difference between PE15 in the chimeric protein and the position in the native protein in binding to MHC class-I and II (Tables 5 and 6).

Table 3 Prediction of binding affinity of TAP binder by TAPPred in STX2a-PE15-P4A8 chimeric protein

Id peptide rank	Start position	Sequence	Score	Predicted affinity
1	62	ARFDHIRIA	10.75	High
2	537	ARAYYGNIY	9.00	High
3	346	SSYSYMHWY	8.88	High
4	538	RAYYGNIYY	8.58	High
5	131	SRHSLVSSY	8.08	High

ABCpred web server was used to predict B-cell linear epitopes of the chimeric and native protein. The best epitopes were obtained according to the criteria based on cutoff values > 0.51. This server predicted 60 and 35 linear epitopes for the chimeric and native protein, respectively (Table 7). 43 and 32 discontinuous B cell epitopes were computed in the chimeric and native protein using Discotope server (Sarkar et al. 2013) with cutoff values > −3.700. In addition, There were no same B cell epitopes in the chimeric and native proteins (Table 8).

Prediction of allergenic and antigenic properties of the chimeric protein

Using Algpred web server, the allergenicity of the chimeric and native protein was calculated 1.00 and 1.35, resistivity. Algpred can be predicted allergens using resemblance of a known epitope with any region of the protein.

VaxiJen web server was used to align independent prediction of protective antigens of tumor bacterial, and viral origin. This server computed the average antigenicity of the STX2a-PE15-P4A8 chimeric construct with 0.66 score, which was higher than the threshold 0.4 (bacteria) and 0.5 (tumor). This score was 0.43 and 0.5 for the native protein (PE38) and a part of the chimeric protein (STX2a-PE15), respectively. The results show that the chimeric and native proteins don't have allergenic properties, but have a little antigenic properties.

Cellular and cytokine responses

C-IMMSIM combines techniques of systems biology with information provided by data-driven prediction methods. The results of B cell populations shows that the B cells isotype IgM are the dominant cells for response to the immunotoxin (Fig. 3a). As shown at Fig. 3b, the most of anti immunotoxin antibodies are IgM isotype antibodies. The prediction of dendritic cells (DCs) shows that the most of them are in the rest state and the response of the NK cells decreases in a 30 days period (Fig. 3c and d). This demonstrates that probably the innate immune

Table 4 Prediction of CTL epitopes on the chimeric protein by NetCTL-1.2 server with threshold 0.75

Position	Sequence	aff*	aff_rescale*	cle*	Tap*	COMB*
527	TSEDSAIYY	0.7402	3.1430	0.9451	2.8480	3.4271
526	LTSEDSAIY	0.6680	2.8363	0.9512	3.0350	3.1307
469	FTDYGMHWV	0.5471	2.3228	0.4527	0.0320	2.3923
346	SSYSYMHWY	0.5247	2.2277	0.9750	3.2150	2.5347
342	SVSTSSYSY	0.4212	1.7883	0.9757	3.2130	2.0953

*aff, Predicted MHC binding affinity (The value is given as 1–log 50 k (aff), where log50k is the logarithm with base 50.000, and aff is the affinity in nM units); aff_rescale, Rescale binding affinity (The predicted binding affinity is normalized by the 1st percentile score); *cle* c terminal cleavage affinity; *Tap* TAP transport efficiency; *COMB* prediction score

Table 5 Predictions of MHC-I for the chimeric protein by IEDB server

Allele	Start	End	Length	Peptide	ic50	Allele	Start	End	Length	Peptide	ic50
HLA-C*03:03	6	14	9	AASASGGPE	1.64	HLA-B*18:01	2	9	8	DEAGAASA	18.59
HLA-C*03:03	12	20	9	FAVDIRGLD	3.41	HLA-C*12:03	10	18	9	SYFAVDIRG	19.51
HLA-C*03:03	11	19	9	YFAVDIRGL	4.63	HLA-C*03:03	4	12	9	NHTPPGSYF	20.59
HLA-C*12:03	3	11	9	EAGAASASG	10.48	HLA-C*12:03	5	13	9	GAASASGGP	23.78
HLA-C*14:02	10	18	9	SYFAVDIRG	11.71	HLA-A*68:02	9	18	10	GSYFAVDIRG	25.72
HLA-C*03:03	8	16	9	PGSYFAVDI	12.32	HLA-C*12:03	6	14	9	TPPGSYFAV	13.84
HLA-C*03:03	3	11	9	EAGAASASG	12.32	HLA-C*12:03	1	9	9	NDEAGAASA	14.30
HLA-C*12:03	5	13	9	HTPPGSYFA	12.57	HLA-C*03:03	2	10	9	DEAGAASAS	14.74
HLA-C*03:03	4	12	9	AGAASASGG	12.93	HLA-C*12:03	6	14	9	AASASGGPE	15.75
HLA-C*03:03	5	13	9	GAASASGGP	12.96	HLA-B*15:02	4	12	9	NHTPPGSYF	26.87
HLA-A*02:06	3	10	8	EAGAASAS	13.13	HLA-C*12:03	3	11	9	INHTPPGSY	28.99
HLA-C*12:03	12	20	9	FAVDIRGLD	13.16	HLA-C*12:03	7	15	9	PPGSYFAVD	29.05
HLA-B*15:01	2	11	10	VINHTPPGSY	13.78	HLA-C*12:03	9	17	9	GSYFAVDIR	31.28
HLA-B*15:02	4	12	9	NHTPPGSYF	26.87	HLA-C*12:03	8	16	9	PGSYFAVDI	32.75
HLA-C*12:03	3	11	9	INHTPPGSY	28.99	HLA-A*02:06	3	10	8	INHTPPGS	35.41
HLA-C*12:03	7	15	9	PPGSYFAVD	29.05	HLA-A*68:02	3	12	10	EAGAASASGG	38.13
HLA-C*12:03	9	17	9	GSYFAVDIR	31.28	HLA-C*12:03	1	9	9	SVINHTPPG	39.65
HLA-C*12:03	2	10	9	VINHTPPGS	31.42	HLA-C*03:03	1	9	9	NDEAGAASA	44.42
HLA-C*03:03	3	11	9	INHTPPGSY		HLA-C*07:02	11	19	9	YFAVDIRGL	47.44
HLA-C*03:03	9	17	9	GSYFAVDIR	47.60						

*The predicted output is given in units of IC_{50}nM, peptides with IC_{50} values < 50 nM are considered high affinity, < 500 nM intermediate affinity and < 5000 nM low affinity. Some epitopes have low affinity, but no known T cell epitope has an IC_{50} value greater than 5000

Table 6 Predictions of MHC-II for the chimeric protein by IEDB server

Allele	Start	End	Core sequence	Peptide sequence	IC50
HLA-HLA-DRB1*03:01	6	14	TPPGSYFAV	TPPGSYFAVDIRGLD	195.00
HLA-HLA-DRB1*01:01	11	19	YFAVDIRGL	TPPGSYFAVDIRGLD	251.00
HLA-HLA-DRB1*01:01	5	13	HTPPGSYFA	HTPPGSYFAVDIRGL	254.00
HLA-HLA-DRB1*07:01	3	11	INHTPPGSY	SVINHTPPGSYFAVD	284.00

system does not form a wide responses against our immunotoxin. Lack of extensive innate immune responses can lead to a smaller humoral and cellular immune response and, more importantly, prevent the formation of memory cells (Rezaie et al. 2019). The cellular immune responses tended to the Th1 so that the INF-g has been produced in greater quantities (Fig. 3e and f).

Docking chimeric protein

The prediction of the chimeric protein interaction with its receptor, Fn14, on the tumor cells was predicted using Hex web server. STX2a-PE15-P4A8 showed high affinity towards the Fn14 receptor with E-total value of the docking complex − 559.58 kcal/mol which predicts the best docking complex with a low E-total value (Fig. 4).

Discussion

Cancer is the most cause of death in the developing countries of the world. Several approaches and methods are designed for the treatment of cancer including chemotherapy, radiation, and surgery or a combination of two or more. Hormones, chemotherapeutic agents and immunotoxins are types of drugs that are used in the treatment of cancer. Immunotoxin is a protein-based therapy, which comprises an antibody or a fragment of antibody that is fused to a bacterial or plant toxin (Cancer 2014; Kreitman 2006; Zauber et al. 2012). Studies have shown that the toxin moieties of immunotoxins, such as *Pseudomonas* exotoxin A (PE), *diphtheria toxin*, and ricin, are able to induce apoptosis. Pseudomonas exotoxin A (PE) is an extremely toxic protein released by the opportunistic

Table 7 The predicted linear B cell epitopes of the chimeric protein by ABCpred

Sequence	Start position	Sequence	Start position
RTEISTPLEHISQGTT	21	GGGSGGGGSQVQLQQS	432
IGVISTYNGYTNYNQK	488	RFVTVTAEEFAGPADS	160
HISQGTTSVSVINHTP	30	LERSGMQISRHSLVSS	123
KGSGYTFTDYGMHWVK	463	FTHISVPGVTTVSMTT	95
AVDIRGLDVYQARFDH	51	YQARFDHLRLIIEQNN	60
GPEVVRPGVSVKISCK	448	GGSQVQLQQSGPEVVR	438
LTSEDSAIYYCARAYY	526	GQRATISCRASKSVST	330
SVSTSSYSYMHWYQQK	342	VALYLAARLSWNQVDQ	237
GEAIREQPEQARLALT	268	GVTTVSMTTDSSYTTL	102
SWNQVDQVIRNALASP	246	QSPASLAVSLGQRATI	320
AGPADSGDALLERNYP	170	RFVRQGTGNDEAGAAS	291
DKSSSTAYMELARLTS	513	AEFLGDGGGSLAALTA	188
HWYQQKPGQPPKLLIK	352	NGYTNYNQKFKGKATM	495
ASASGGPEKLDIVLTQ	305	GVSVKISCKGSGYTFT	455
AYYGNLYYAMDYWGQG	539	QACHLPLETFTRHRQP	205
GGGGSGGGGSGGGGSQ	426	TNTFYRFSDFTHISVP	86
GFVNTATNTFYRFSDF	80	DFILNIHPVEEEDAAT	388
KFKGKATMTVDKSSST	503	LESGVPARFSGSGSGT	372
QHSRELPFTFGSGTKL	407	TLAAAESERFVRQGTG	283
VSVINHTPPGSYFAVD	38	TRHRQPRGWEQLEQCG	215
TIDFSTQQSYVSSLNS	4	HSLVSSYLALMEFSGN	133
MEFSGNTMTRDASRAV	143	QVIRNALASPGSGGDL	252
ARFSGSGSGTDFILNI	378	GWEQLEQCGYPVQRLV	222
PGSGGDLGEAIREQPE	261	TLQRVAALERSGMQIS	116
GGSLAALTAHQACHLP	195	NNLYVAGFVNTATNTF	74
TMTRDASRAVLRFVTV	149	YYAMDYWGQGTSVTVS	545
RLIIEQNNLYVAGFVN	68	KLDIVLTQSPASLAVS	313
PVEEEDAATYYCQHSR	395	YGMHWVKQSHAKSLEW	472
ALLERNYPTGAEFLGD	178	GQPPKLLIKYASNLES	359
TDSSYTTLQRVAALER	110	QSYVSSLNSIRTEIST	11

Table 8 Prediction of discontinuous B-cell epitopes in the chimeric protein based on Discotope server

Number	Amino acid	Score	Sensitivity	Specificity
359	GLY	0	2.598	2.299
360	GLN	13	1.907	0.193
361	PRO	3	1.459	0.946
434	GLY	9	1.243	0.065
435	SER	5	0.611	− 0.034
129	GLN	3	− 1.837	− 1.971

pathogen *Pseudomonas aeruginosa*, and because of the low immunogenic than other toxins is used in the treatment. In addition, modular structure and function's mechanism of PE make it subject to wide variations which can redirect its strong cytotoxicity from disease to cure diseases. In combination with various synthetic targets such as antibody fragments, PE becomes a drug of choice to eliminate specific cell populations (Pastan et al. 2006; Weldon and Pastan 2011). Shiga like toxin is another toxin that can induce apoptosis. Stx includes two major antigenic forms (Stx1 and Stx2), with different variants of Stx2 (Stx2a to -h) that Stx2a is more potent than Stx1 (Binnington et al. 2002). Ligand targeted therapy (LTT) is a potent medicinal strategy to deliver a selective drug to targeted cells, for limiting side effects and toxicity. LTT is used in the treatment of various diseases such as cancer (Kreitman 2006; Trapani et al. 2012; Wu et al. 2006).

Fn14 receptor is expressed in low quantity in normal tissues, but is clearly important in injured tissues. Therefore, Fn14 is overexpressed in breast, brain, esophageal, prostate, gastric and bladder cancers, and it may act as an aggressive role in these conditions (Brown et al. 2003; Winkles 2008; Zhou et al. 2011). Herein, we selected the Fn14 receptor for binding to its ligand (anti Fn14 or P4A8) that is fused to STX2a-PE15 as a new anti-tumor drug. The structures, physicochemical properties, stability, epitope mapping and

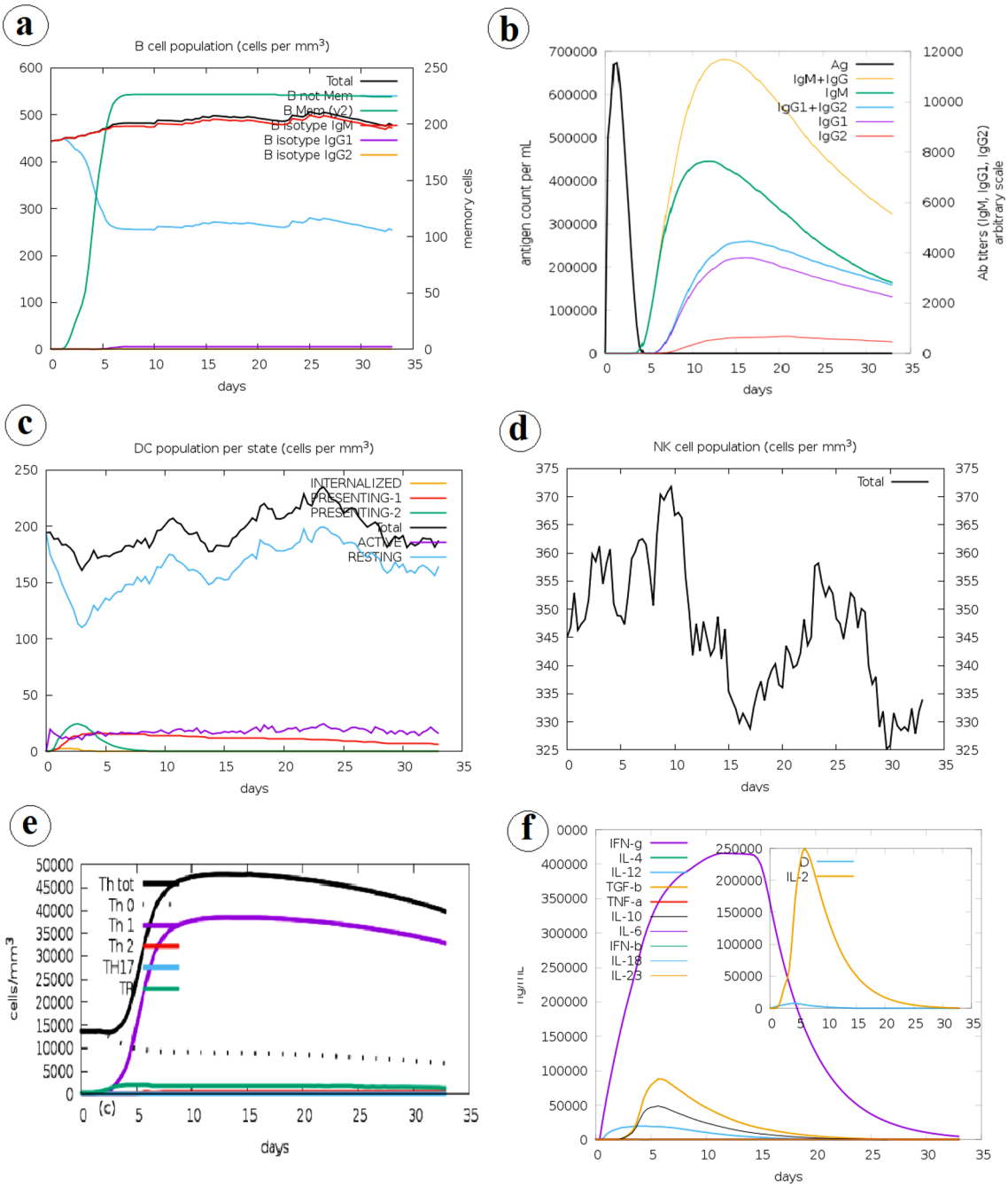

Fig. 3 Cellular and cytokine responses to immunotoxin. **a** B cells responses; **b** Antibody response; **c** responsive DC populations; **d** responsive NK cells populations; **e** T cells response; **f** cytokine reponse. All cellular and cytokine responses have been predicted in a 30 days period

ligand-receptor relevance of this chimeric protein compared to native protein were computed by bioinformatic servers or tools.

Codon adaptation index (CAI) with a range of 0–1 used to measure the deviation of the desired protein coding gene sequence. In addition, it is applied for a reference set of genes and estimate the level of its expression (Carbone et al. 2003). Afterward, we selected a bacterial host (*Escherichia coli*) as an expression vector to express the *stx2a-pe15-p4a8* gene. CAI index of the STX2a-PE15-P4A8 protein was improved from 0.68 to 0.93. Furthermore, the GC content was reduced from 56.3% to 52.9%. Since, the expression is higher when CAI is nearer to 1, that the STX2a-PE15-P4A8 has a high expression level in *E.coli*. Also, the reduction of GC% represents the stability of chimeric gene's mRNA.

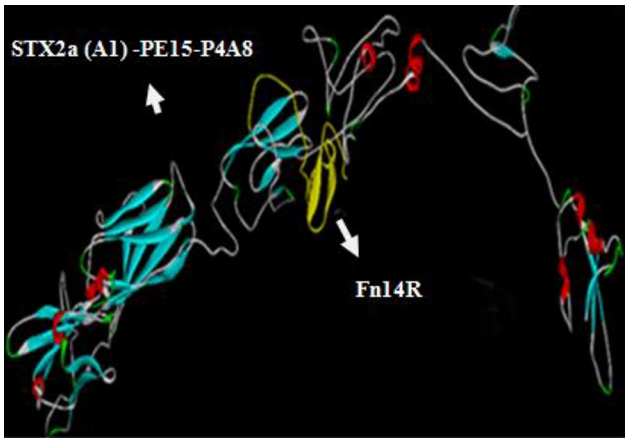

Fig. 4 Protein-substrate interaction. Schematic view of docking model between STX2a (A1) -PE15-P4A8 ligand and Fn14 receptor. Fn14 receptor marked with yellow color

Mfold is a useful web server for predicating mRNA structure based on a theoretically tractable DP algorithm. It can search the minimum ΔG structure in its thermodynamic model and high capacity to predict true positive base pairs (Zuker 2003). Our results showed that the mRNA is sufficiently stable for efficient translation in the prokaryotic host.

ProtParam is a tool that uses for the computation of several physical and chemical parameters for the desired protein (Amala 2010). The primary structure analysis of the STX2a-PE15-P4A8 chimeric protein showed that it is naturally hydrophilic because of having the high levels of polar residues. The presence of 10 Cys residues in the STX2a-PE15-P4A8 chimeric protein resulted in conformation of disulphide bridges (SS bonds) in this chimeric protein. Disulfide bonds act a significant role in the folding and stability of some proteins, specific secretory proteins (in prokaryotic or eukaryotic host). Moreover, this server predicated the average molecular weight of the STX2a-PE15-P4A8 chimeric protein about 60.7 kDa. Protein isoelectric point (pI) is computed through pKa values of amino acids. The pKa value of amino acids relates to its side chain and has a significant role in defining the pH dependent specifications of a protein. The acidity of the chimeric protein was identified by pI value 6.13. The pI showed the pH of the chimeric protein surface is positive. The high number of negatively charged amino acids (Asp + Glu = 55) versus positively charged amino acids (Arg + Lys = 44) is the main contributing factor to the negative charge. At acidic pI, proteins are stable; so this parameter may be helpful to develop buffer systems for purification of this protein using isoelectric focusing techniques.

Although Expasy's ProtParam computes the extinction coefficient; It demonstrates how much light a protein is absorbed at a specific wavelength (Amala 2010). The extinction coefficient of the STX2a-PE15-P4A8 at 280 nm is 76585 M^{-1} cm^{-1} due to the high concentration of Cys, Trp and Tyr. The extinction coefficient is to measure protein concentration needed for quantitative study of protein–protein and protein–ligand interactions in solutions. The half-life is the time that protein takes for disappearing its half of amount after its synthesis in cells. The bio computed half-life of the STX2a-PE15-P4A8 is more than 10 h. The instability index can predicate stability of the desired protein in a test tube. Instability index of the STX2a-PE15-P4A8 chimeric protein is more than 40 and it is predicted as unstable. The aliphatic index of a protein is depicted as the relative volume occupied using the amino acids like alanine, valine, isoleucine and leucine. Aliphatic index is considered as a positive factor to increase thermal stability of spherical proteins and ranged from 76.24 to 96.31. The lower thermal stability of the STX2a-PE15-P4A8 chimeric protein is indicative of a perfected elastic structure when associated with a highly aliphatic index, which presumes strength for a broad spectrum of temperature. The GRAVY value of a protein is computed by the addition of the hydropathy values to every amino. Increasing a positive score displays a higher hydrophobicity. Grand average hydropathy (GRAVY) index of the STX2a-PE15-P4A8 chimeric protein is − 0.286. This issue indicates that it's hydrophilic. The very low GRAVY index of this chimeric protein shows that the STX2a-PE15-P4A8 chimeric protein can be produced in a better interface with water. It can be concluded that the physico-chemical properties of the chemical protein are approximately similar to native protein.

As native protein, the chimeric protein has low solubility chance and shows that it can't be purified under normal conditions when overexpressed in *E. coli.* The secondary structure of the chimeric protein is predicted by GOR IV (Sen et al. 2005). Our results showed that random coil is mainly, followed by alpha helix and extended strand like native protein. It seems that the high coil structural content of the STX2a-PE15-P4A8 chimeric protein is due to the high rate of glycine and proline amino acids. Proline has a particular character in production of polypeptide chain twists by disruption of given secondary structure.

The three-dimensional (3D) structural details of proteins are important in determining their molecular function significantly. Moreover, the prediction of the 3D structures will help in the reorganization of binding sites and may result in designing the new drugs. The prediction of the 3D model of the STX2a-PE15-P4A8 chimeric protein was done by I-TASSER server (Zhang 2008). This server produced five models with several C-Scores. Among the five models, the model 5 with the highest C-Score was chosen as the best model and chosen for further analysis. Subsequently, producing 3D models, structural assessment and stereo chemical analyses were done by Ramachandran plot (Lovell et al. 2003). Visualizer and ActiveX Control 4.0 software used to

detect energy minimization. In Ramachandran plot analysis, the allowed φ, ψ backbone conformational regions in the chimeric and native protein were approximately the same, and both proteins are stable. Identification of allergic probability is a main topic whenever new proteins, in contact with humans, either via new drugs or other products. Databases and computational tools are highly significant in the evaluation of allergenicity and allergic cross-reactivity. We used of the AlgPred web server for identification of antigenic proteins (Ivanciuc et al. 2003). Both proteins (STX2a-PE15-P4A8 and PE38) didn't have allergenic characterization. For designing of new drugs, prediction of antigenic epitopes on the protein is very important. VaxiJen web server was used for predicting antigenic properties of the chimeric and native protein based on the physico-chemical properties (Doytchinova and Flower 2008). The results showed that the chimeric and native proteins probably have antigenic properties.

MHC binding is the best indicator of immunogenicity and prediction of the cleavage site. There are several servers that predict MHC class I pathways like proteasomal cleavage and TAP transport efficiency. Prediction of the cleavage sites of the human proteasome in the STX2a-PE15-P4A8 chimeric protein was done by NetChop server (Nielsen et al. 2005). It predicted that the STX2a fragment contained a high amount of cleavage positions. TAPPred server (Bhasin and Raghava 2004a) was used for the prediction of binding affinity in the chimeric protein versus native protein. The prediction of TAP binding peptides is essential to identify the MHC class-1 restricted T cell epitopes (Bhasin and Raghava 2004a). There were 35 and 11 TAP binding sequences with high affinity in the chimeric and native protein, respectively, and only five TAP binding sequences of the chimeric protein were similar to the TAP binding sequence of the native protein. It can be concluded that the chimeric protein is able to stimulate more T-cells.

Another proteasome system is NetCTL 1.2 server that predicts CTL epitopes in the chimeric protein sequence (Larsen et al. 2007). CTLs identify small peptides with length of eight to ten amino acids (Bhasin and Raghava 2004b). This server predicted that there are only two same MHC ligands in PE38 and STX2a-PE15-P4A8 chimeric protein. IEDB server is widely used for prediction of MHC class I and II binding, and prediction of HLA-class I binders, especially for identification of HLA-A*0201 restricted epitopes (Zhang et al. 2008). As we know, MHC I only present intracellular antigen to T cells and evoke cell mediated immunity. In contrast, humoral immunity by forming anti-immunotoxin antibodies can reduce the serum half-life and inhibits cytotoxicity of immunotoxins. Nevertheless, as the results showed, the STX2a-PE15-P4A8 does not bind widely to the MHC class II molecules. Thus, possibility of induction of potent humoral immunity, resulting in the formation of anti-immunotoxin antibodies is low. Using a less immunogenic form of the PE toxin (PE15) has the main role in causing such advantage.

ABC pred was used for prediction of linear epitopes in the chimeric and native protein (Saha and Raghava 2006).

There are 13 same linear B cell epitopes in PE38 and STX2a-PE15-P4A8 chimeric protein with the score > 0.51. In addition, DiscoTope server predicts discontinuous B cell epitopes from proteins (Kringelum et al. 2012). It predicted 43 discontinuous epitopes in the STX2a-PE15-P4A8 chimeric protein that 32 B cell epitopes belong to STX2a. There were no discontinuous B cell epitopes in PE15 fragment. while 5 of 32 B cell epitopes in PE38 belong to Ia and II domains of PE38. These results indicated that Stx2A of the chimeric protein is more antigenic than PE38 alone and can bind to B cells receptors. Although, in accorfing to that this protein cannot display by MHCII, it seems could not stimulate humoral immunity.

Hex server used to assess the interaction of the STX2a-PE15-P4A8 chimeric protein as ligand with Fn14 as receptor (Yaraguppi et al. 2021). Our results showed that the binding ability of the STX2a-PE15-P4A8 is extreme enough to its receptor (Fn14). Thus, the STX2a-PE15-P4A8 chimeric protein may be a new antitumor candidate in cancer immunotherapy.

Conclusions

Our findings suggested that the STX2a-PE15-P4A8 chimeric protein can be as a new antitumor candidate, especially when the targeted mutation is used to reduce the immunogenicity of STX2a (A1). In addition, our results showed that STX2A-PE15-P4A8 chimeric protein is as stable as PE38 protein.

Supplementary Information The online version contains supplementary material available at https://doi.org/10.1007/s40203-021-00079-w.

Author contributions MK, JA, and JF designed the chimeric protein for the article. MK, ER and JA assessed the chimeric protein through various bioinformatic softwares and drafted the early version of the manuscript. MD and JF evaluated and discussed the software and the results. MD, ER and JF provided comments on the manuscript and contributed to editing of the manuscript. MD received the grant for the current study. All authors read and approved the final manuscript.

Funding This study is part of a research project with Grant No. 29903 that supported by Tehran University of Medical Sciences & Health Services.

Data availability All data analyzed during this study are included in this article.

Compliance with ethical standards

Conflict of interest The authors declare that they have no competing interests.

References

Alewine C, Hassan R, Pastan I (2015) Advances in anticancer immunotoxin therapy. Oncologist 20:176

Amala S (2010) In silico analysis and 3D modeling of ASAH1 protein in farber. Lipogranulomatosis 10:06–08

Bhasin M, Raghava G (2004a) Analysis and prediction of affinity of TAP binding peptides using cascade SVM. Protein Sci 13:596–607

Bhasin M, Raghava G (2004b) Prediction of CTL epitopes using QM SVM and ANN techniques. Vaccine 22:3195–3204

Binnington B, Lingwood D, Nutikka A, Lingwood CA (2002) Effect of globotriaosyl ceramide fatty acid α-hydroxylation on the binding by verotoxin 1 and verotoxin 2. Neurochem Res 27:807–813

Brown S, Richards C, Hanscom H, Feng S, Winkles J (2003) The Fn14 cytoplasmic tail binds tumour-necrosis-factor-receptor-associated factors 1, 2, 3 and 5 and mediates nuclear factor-kappaB activation. Biochem J 371:395–403

Cancer IAfRo (2014) GLOBOCAN 2012: estimated cancer incidence, mortality and prevalence worldwide in 2012 World Health Organization. https://www.iarc.who.int/news-events/latest-world-cancer-statistics-globocan-2012-estimated-cancer-incidence-mortality-and-prevalence-worldwide-in-2012/

Carbone A, Zinovyev A, Képès F (2003) Codon adaptation index as a measure of dominating codon bias. Bioinformatics 19:2005–2015

Doytchinova IA, Flower DR (2008) Bioinformatic approach for identifying parasite and fungal candidate subunit vaccines. Open Vaccine J 1:22–26

Hassan R et al (2014) Phase 1 study of the antimesothelin immunotoxin SS1P in combination with pemetrexed and cisplatin for front-line therapy of pleural mesothelioma and correlation of tumor response with serum mesothelin, megakaryocyte potentiating factor, and cancer antigen 125. Cancer 120:3311–3319

Ivanciuc O, Schein CH, Braun W (2003) SDAP: database and computational tools for allergenic proteins. Nucl Acids Res 31:359–362

Kawa S, Onda M, Ho M, Kreitman RJ, Bera TK, Pastan I (2011) The improvement of an anti-CD22 immunotoxin. MAbs 3(5):479–486

Keshtvarz M et al (2017) Bioinformatic prediction and experimental validation of a PE38-based recombinant immunotoxin targeting the Fn14 receptor in cancer cells. Immunotherapy 9:387–400

Kreitman RJ (2006) Immunotoxins for targeted cancer therapy. AAPS J 8:E532–E551

Kringelum JV, Lundegaard C, Lund O, Nielsen M (2012) Reliable B cell epitope predictions: impacts of method development and improved benchmarking. PLoS Comput Biol 8:e1002829

Larsen MV, Lundegaard C, Lamberth K, Buus S, Lund O, Nielsen M (2007) Large-scale validation of methods for cytotoxic T-lymphocyte epitope prediction. BMC Bioinform 8:424

Lovell SC et al (2003) Structure validation by Cα geometry: ϕ, ψ and Cβ deviation proteins: structure. Funct Bioinform 50:437–450

Matar AJ et al (2012) Effect of pre-existing anti-diphtheria toxin antibodies on T cell depletion levels following diphtheria toxin-based recombinant anti-monkey CD3 immunotoxin treatment. Transpl Immunol 27:52–54

Michalska M, Wolf P (2015) *Pseudomonas exotoxin* A: optimized by evolution for effective killing. Front Microbiol 6:963

Nielsen M, Lundegaard C, Lund O, Keşmir C (2005) The role of the proteasome in generating cytotoxic T-cell epitopes: insights obtained from improved predictions of proteasomal cleavage. Immunogenetics 57:33–41

Pastan I, Hassan R, FitzGerald DJ, Kreitman RJ (2006) Immunotoxin therapy of cancer. Nat Rev Cancer 6:559–565

Rezaie E et al (2019) Different frequencies of memory B-cells induced by tetanus, botulinum, and heat-labile toxin binding domains. Microb Pathog 127:225–232

Rezaie E, Bidmeshki AP, Amani J, Mahmoodzadeh Hosseini H (2020a) Bioinformatics predictions, expression, purification and structural analysis of the PE38KDEL-scfv immunotoxin against EPHA2 receptor. Int J Pept Res Ther 26:979–996. https://doi.org/10.1007/s10989-019-09901-8

Rezaie E, Amani J, Pour AB, Hosseini HM (2020b) A new scfv-based recombinant immunotoxin against EPHA2-overexpressing breast cancer cells. High in vitro anti-cancer potency. Eur J Pharmacol 870:172912

Saha S, Raghava G (2006) Prediction of continuous B-cell epitopes in an antigen using recurrent neural network proteins: structure. Funct Bioinform 65:40–48

Sarkar A, Banik A, Pathak BK, Mukhopadhyay SK, Chatterjee S (2013) Envelope protein gene based molecular characterization of Japanese encephalitis virus clinical isolates from West Bengal, India: a comparative approach with respect to SA14–14–2 live attenuated vaccine strain. BMC Infect Dis 13:368

Sen TZ, Jernigan RL, Garnier J, Kloczkowski A (2005) GOR V server for protein secondary structure prediction. Bioinformatics 21:2787–2788

Siegel RL, Miller KD, Jemal A (2019) Cancer statistics, 2019. Cancer J Clin 69:7–34

Trapani G, Denora N, Trapani A, Laquintana V (2012) Recent advances in ligand targeted therapy. J Drug Target 20:1–22

Tredget EE, Shankowsky HA, Rennie R, Burrell RE, Logsetty S (2004) *Pseudomonas* infections in the thermally injured patient. Burns 30:3–26

Weldon JE, Pastan I (2011) A guide to taming a toxin–recombinant immunotoxins constructed from *Pseudomonas exotoxin* A for the treatment of cancer. FEBS J 278:4683–4700

Whitsett TG et al (2012) Elevated expression of Fn14 in non-small cell lung cancer correlates with activated EGFR and promotes tumor cell migration and invasion. Am J Pathol 181:111–120

Winkles JA (2008) The TWEAK–Fn14 cytokine–receptor axis: discovery, biology and therapeutic targeting. Nat Rev Drug Discov 7:411–425

Wu H-C, Chang D-K, Huang C-T (2006) Targeted therapy for cancer. J Cancer Mol 2:57–66

Yaraguppi DA, Udapudi BB, Patil LR, Hombalimath V, Shet AR (2021) IN-silico analysis for predicting protein ligand interaction for snake venom protein. J Adv Bioinfo Res 3:345–356

Zauber AG et al (2012) Colonoscopic polypectomy and long-term prevention of colorectal-cancer deaths. N Engl J Med 366:687–696

Zhang Y (2008) I-TASSER server for protein 3D structure prediction. BMC Bioinform 9:40

Zhang Q et al (2008) Immune epitope database analysis resource (IEDB-AR). Nucl Acids Res 36:W513–W518

Zhou H, Marks JW, Hittelman WN, Yagita H, Cheung LH, Rosenblum MG, Winkles JA (2011) Development and characterization of a potent immunoconjugate targeting the Fn14 receptor on solid tumor cells. Mol Cancer Ther 10:1276–1288

Zuker M (2003) Mfold web server for nucleic acid folding and hybridization prediction. Nucl Acids Res 31:3406–3415